

F. L. Amorim

Pontifical Catholic University of Paraná – PUC/PR
Department of Mechanical Engineering
Laboratory of Machining Processes - LAUS
Rua Imaculada Conceição, 1155 – Prado Velho
80215-901 Curitiba, PR. Brazil
famorim@rla01.pucpr.br

W. L. Weingaertner

Federal University of Santa Catarina – UFSC
Department of Mechanical Engineering – EMC
88010-970 Florianópolis, SC. Brasil
wlv@emc.ufsc.br

Die-Sinking Electrical Discharge Machining of a High-Strength Copper-Based Alloy for Injection Molds

High-strength copper alloys are used as materials for injection molding tools or as cores and inserts in steel molds because of their high thermal conductivity, corrosion and wear resistance. Unfortunately, there is little technological knowledge on the electrical discharge machining (EDM) of copper-beryllium ASTM C17200 alloy. In this work, rough and finish machining conditions were tested using copper and tungsten-copper as materials for the electrodes. Cross-sectional micrographic and hardness examinations as well as surface roughness measurements were also carried out on workpieces after machining in order to study the thermally affected zones. Appropriate parameters settings for EDM of the investigated alloy are suggested.

Keywords: Die-sinking EDM, copper-beryllium alloy, machining parameters

Introduction

The electrical discharge machining (EDM) is one of the major manufacturing processes widely applied in die and mold making industry to generate deep and three-dimensional complex cavities in many different classes of materials under roughing and finishing operations.

The best supported theory to the explanation of electrical discharge machining process is the thermoelectric phenomenon and according to Van Dijck et al. (1974) and other researchers such as Zolotych (1955), Crookall and Khor (1974), Dibitonto et al. (1989) and König and Klocke (1997) the material removal in electrical discharge machining is associated with the erosive effect produced when spatially and discrete discharges occur between two electrical conductive materials. Sparks of short duration are generated in a liquid dielectric gap separating tool and workpiece electrodes. The electrical energy released by the generator is responsible to melt a small quantity of material of both electrodes by conduction heat transfer. Subsequently, at the end of the pulse duration a pause time begins and forces that can be of electric, hydrodynamic and thermodynamic nature remove the melted pools.

Figure 1, adapted from König and Klocke (1997), presents the phases of a discharge in EDM process. The first one is the ignition phase, which represents the lapse corresponding to the occurrence of the breakdown of the high open circuit voltage \hat{u}_i applied across the working gap until the fairly low discharge voltage u_e , which ranges normally from 15 to 30 V. This period is known as ignition delay time t_d [μ s]. The second phase, which instantaneously occurs right after the first one when the current rapidly increases to the operator specified peak current \hat{i}_e [A], is the formation of a plasma channel surrounded by a vapor bubble. The third phase is the discharge phase; when the high energy and pressure plasma channel is sustained for a period of time t_c [μ s] causing melting and evaporation of a small amount of material in both electrodes. It is important to remark that little evaporation occurs due to the high plasma pressure. The fourth and last one phase is the collapse of the plasma channel caused by turning off the electric energy, which causes the molten material to be violently ejected. At this time, known as interval time t_o [μ s], a part of the molten and vaporized material is flushed away by the flow of the dielectric across the gap

and the rest is solidified in the recently formed crater and next to the surroundings. During the interval time t_o also occurs cooling of the electrodes and the de-ionization of the working gap necessary to promote an adequate dispersion of the successive discharges along the surfaces of the electrodes.

As remarked by Klocke (1998), at present the utilization of new materials for the production of injection molding tools, such as high-strength aluminum alloys and copper-based alloys, represents potential sources for cost reduction of the process. Although, in the case of copper alloys, the purchase price is about a tenfold higher than that of the traditional steels, the overall cost-effectiveness of the process is increased, because the number of possible shots is tripled.

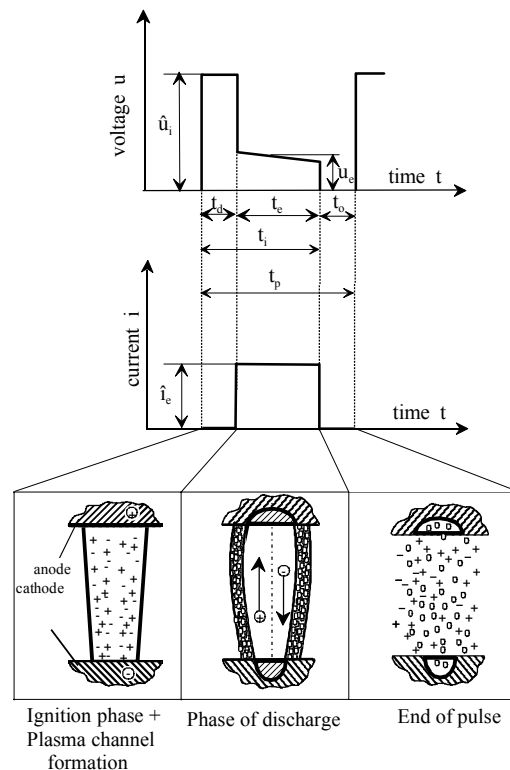


Figure 1. The phases of electric discharge in EDM.

Engelman & Dealey (2000) report that the alloys ASTM C17200, C17510 and C18000 have been especially recognized as excellent materials for injection molding tools or as cores and inserts for steel moulds. The high thermal conductivity of those alloys, normally three to four times higher than that of steel, ensures not only a reduction of the cooling phase of the molding process, but also promotes a better workpiece dimensional control with less tolerance deviation and less warpage, fewer molded-in stresses and a reduced incidence of sink marks. Additional advantages of these alloys also include both good wear and corrosion resistance against many plastic resins normally used in molding industry.

According to Guha et al. (1995) due to the high thermal conductivity of the copper-beryllium ASTM C17200 alloy compared to steel, the adequate machining settings are not the same for those two materials. The present work is focused in assessing the general rough and finish EDM behavior of C17200 alloy in terms of the following technological results:

(1) Material removal rate V_w , which means the volume of material removed from the workpiece per unit time.

(2) Volumetric relative wear \mathcal{G} , which means the ratio of electrode wear rate V_e to material removal rate, expressed as percentage.

(3) Surface texture of the machined workpieces using the Surtronic 3 Taylor Hobson roughness measurement equipment. The measurements were carried out three times on the bottom of the EDM cavity using a stylus tip of 5 μm radius, the cut-off length of 0,8 mm and evaluation length of 4,0 mm.

In EDM the material removal is primarily based on a thermal principle, which directly influences the chemical, physical and micro structural characteristics of the superficial zones of the material, and consequently have important effects on the functionality of workpieces. Plastic injection molds are generally characterized by being exposed to chemical and abrasive wear during the molding cycle.

In this work cross-sectional micrographic and hardness examinations as well as surface roughness measurements were carried out on workpiece samples after machining in order to study the heat affected zone. The main purpose was to observe whether significant differences between CuBe alloy and steel concerning the EDM material removal process and the superficial formation of the part would exist or not.

The basic constituents of the CuBe C17200 alloy are the following: 1,6 to 2,0% Be, Co+Ni 0,3% and the balance Cu of 98%. According to Stonehouse (1986) the only potential problem when manipulating the element beryllium is the inhalation of excessive amounts of respirable beryllium, which means particles with a size smaller than 10 μm . Furthermore, he also remarks that physiological reaction to beryllium exposures appear to be a matter of individual susceptibility, and that the majority of people apparently do not seem to react adversely to exposures at any level. The recommendation of ACGIH (1995) is that any machining process should be accomplished under a wet environment to control beryllium particulate at source. The Die-Sinking EDM is executed with the two electrodes submerged in a dielectric media with an exhaust system installed at the machine, which reduces or even avoid the possibility of the presence of airborne beryllium.

Nomenclature

- \hat{i}_e = discharge current, A
 p_{in} = dielectric inlet pressure, Pa
 t_d = ignition delay time, μs
 t_c = discharge duration, μs
 t_i = pulse duration, μs
 t_0 = pulse interval time, μs

- t_p = pulse cycle time, μs
 u_e = discharge voltage, V
 \hat{u}_i = open circuit voltage, V
 V_e = electrode wear rate, mm^3/min
 V_w = material removal rate, mm^3/min

Greek Symbols

- τ = duty factor, dimensionless
 \mathcal{G} = volumetric relative wear, ration V_e/V_w

Subscripts

- d = relative do ignition delay time
 e = relative to discharge
 i = relative to pulse duration
 in = relative to inlet pressure
 0 = relative to interval time
 w = relative to workpiece

Experimental Procedure

The Electrical Discharge Machining experiments were conducted at the Institute of Machine Tools and Production Engineering at Aachen University of Technology, Germany. A DECKEL DE-10 CNC machine equipped with an isofrequent generator, which means that the pulse duration t_i is set constant, was used to perform the tests.

The workpieces were square specimens 20 mm wide and 5 mm thick, with a roughness R_a of 2 μm on the surface to be machined. Electrolytic copper and tungsten-copper cylindrical bars 100 mm long with a diameter of 15 mm were mounted axially in line with workpieces and used as tool electrodes at positive polarity, as shown in Fig. 2.

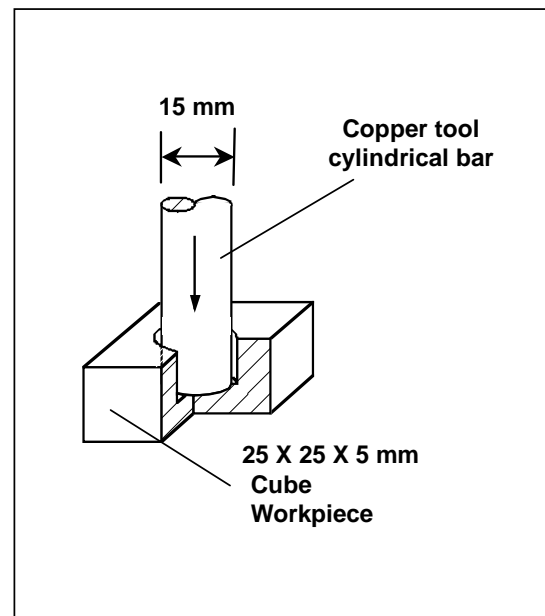


Figure 2. Geometry of the tool electrode and the workpiece.

A lateral flushing which was able to keep a stable process, was applied using the hydrocarbon OEL-HELD IME 82 with 3 cSt of viscosity as the dielectric fluid. The open circuit voltage of 220 V maintained a good stability of the process and was established after pre-tests with $\hat{u}_i = 120$ and 160 V. The accurate quantification of V_w and \mathcal{G} was possible by using a precise scale (resolution = 0,0001 g) to weigh the electrodes before and after an average machining time of 20 minutes.

At the first series of tests, the pulse duration t_i and the peak discharge current \hat{i}_e were varied, so that it could be possible to scan the general machining behavior of the C17200 alloy. The duty factor τ , which means the ratio between the pulse duration t_i and the pulse cycle time t_p , was maintained constant at 0,5 to assure the stability of the process, avoiding the formation of arcing. The settings established for the roughing and finishing regimes are presented in Tab 1.

Table 1. Experimental Machining Settings.

Discharge Current - \hat{i}_e [A]	Pulse duration - t_i [μ s]
21, 40, 64	10, 30, 100, 300, 500, 600
4, 8, 15	8, 10, 20, 30, 100, 300, 500

The second series of tests aimed the optimization of the values of V_w and ϑ . The duty factor was then varied from 0,5 up to 0,97, using the optimum pulse durations achieved for $\tau = 0,5$.

At the sequence, the electrical discharge machined surfaces of the samples were analyzed using scanning electron microscope. After embedded in epoxy and polished, the samples were etched with ammonium persulfate/ammonium hydroxide and micrographic

examinations were performed with optical microscopy technique in order to examine the heat affected zone and the existence and distribution of micro cracks and pores. Micro hardness (HV) measurements were also carried out to investigate the thermal effects of EDM on C17200 alloy.

Results and Discussions

In Fig. 3 and Fig. 4, respectively for copper and tungsten-copper tool electrodes, the workpiece material removal rate V_w and the volumetric relative wear ϑ are plotted versus the pulse duration t_i and the discharge current \hat{i}_e for rough machining conditions. From the diagrams it can be clearly noticed that as the pulse duration t_i increases, V_w also increases up to a maximum value for a specific optimum t_i . Beyond this point V_w starts decreasing rapidly. The explanation for V_w behavior after its maximum point is concerned to the very high plasma diameter expansion, due to the long pulse duration t_i , that diminishes pressure and energy of the plasma channel over the molten material of the electrodes. As a consequence this phenomenon brings instability to the process lowering the material removal rate.

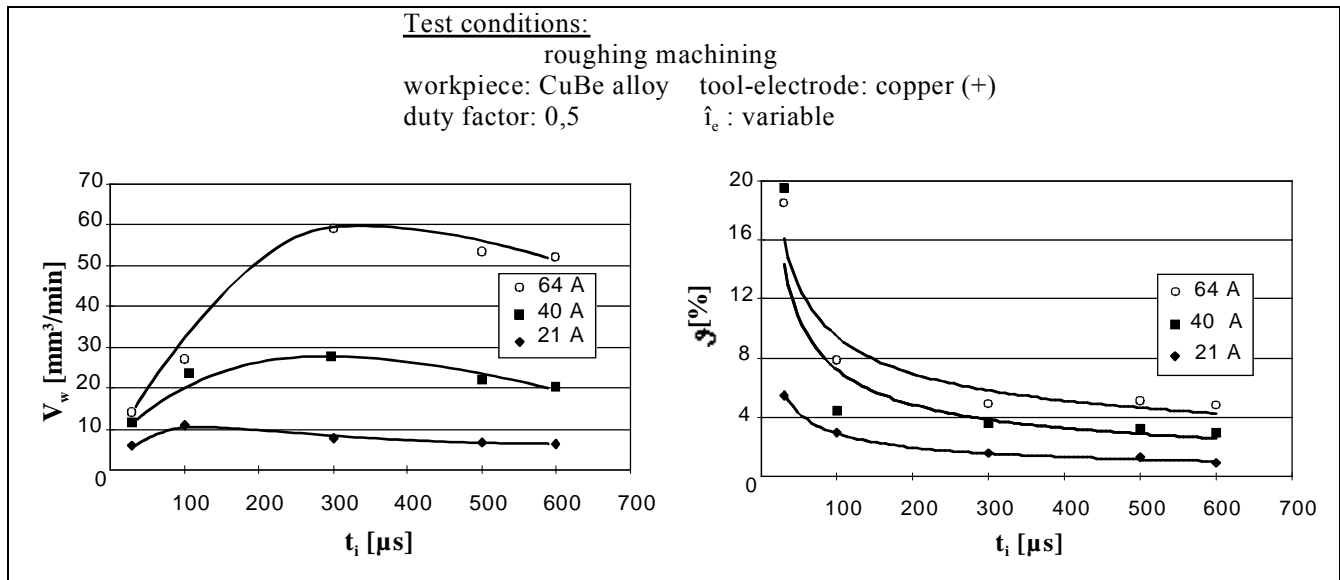


Figure 3. Results of the roughing experiments for the copper electrodes.

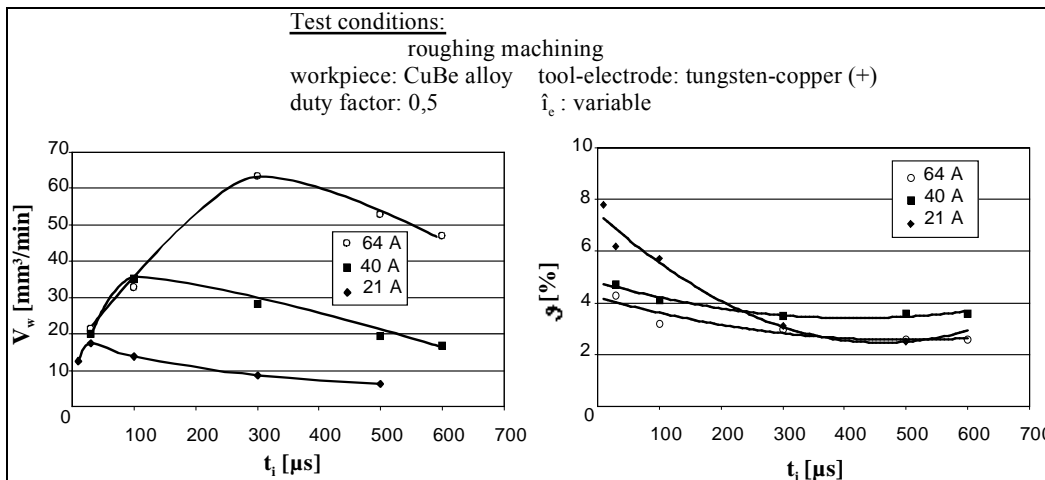


Figure 4. Results of the roughing experiments for the tungsten-copper electrodes.

Invariably for rough and finish EDM, when applying a duty factor of 0,5, the best rates of material removal rate V_w were obtained for tungsten-copper electrodes. In this case, the maximum value reached for V_w was 63,5 mm³/min at $i_e = 64$ A and $t_i = 300$ μ s.

When machining with copper electrodes, it is observed that higher is the discharge current i_e higher is the relative wear ϑ . For tungsten-copper electrodes, a contrary response appears, it means, increasing the discharge current i_e decreases the volumetric relative wear ϑ .

The volumetric relative wear ϑ (V_e/V_w) is given by the ratio between the electrode wear rate V_e and material removal rate V_w . According to Drozda (1983) generally the electrode wear rate V_e is lower for materials with high melting and boiling points, among other properties.

So, the higher melting point of tungsten-copper (W-Cu) in comparison to the one of electrolytic copper has promoted better resistance of W-Cu electrode against the thermally influenced wear. Thus, the lower levels of relative wear ϑ for EDM with W-Cu electrodes, as discharge current increases, is related to this property which has caused a lesser level of V_e in comparison to the one achieved with electrolytic copper.

In order to keep a stable machining process regarding aspects such as a proper dispersion of discharges along the frontal area of the electrodes, an uniform tool electrode wear, a good de-ionization of the dielectric and an adequate flushing of debris, so that any excessive adhesion of particles from the workpiece or dielectric byproducts be observed on the bottom of the tool electrode, is recommended to accomplish the machining under the following settings to consequently attain the best results of material removal rate and the surface roughness:

- a) $i_e = 40$ and 64 A, the use of $t_i = 300$ μ s gives the best results;
- b) $i_e = 21$ A, the application of $t_i = 100$ μ s and $t_i = 30$ μ s respectively for copper and tungsten-copper electrodes;
- $i_e = 4, 8$ and 15 A, the value of $t_i = 30$ μ s is suitable for both materials of tool electrodes.

It is important to remark that depending on the electrode geometry, the flushing conditions and the model of the machine, different results from those obtained in this work can be achieved. Thus, the settings established above should be taken only as guidelines for EDM of CuBe C17200 alloy.

Normally, high values of duty factor τ increase the material removal rate V_w - the volume of material removed from the workpiece per unit of time [mm³/min] - and, consequently, decrease the volumetric relative wear ϑ (V_e/V_w), as depicted in Fig. 5.

The duty factor τ (t_i/t_p), which means the ratio between the pulse duration t_i and the pulse cycle time t_p ($t_p = t_i + t_o$), may be controlled adjusting the interval time t_o between two successive pulses. The high values of duty factor is commonly established by keeping t_i constant and decreasing the value of t_o . This procedure causes the elevation of discharges frequency ($f = 1/t_p$), which promotes an increase of material removal rate V_w and the reduction of the relative wear ϑ (V_e/V_w).

The initial test were carried out with a duty factor $\tau = 0,5$, i.e., $t_i = t_o = 300$ μ s, because the good stability normally observed on EDM operations for this condition, which means a few occurrence of short-circuits and arc-discharges as a consequence of the proper flushing of eroded particles away from the working gap. Smaller values of duty factor ($t_i < t_o$) were avoided because it would lead to very low discharges frequency, consequently decreasing the material removal rate V_w . On the other hand, very high levels of τ ($t_i > t_o$) would probably cause an over-concentration of debris in the working gap leading to non-uniform material removal rate V_w .

As shown in Fig. 5a, the maximum duty factor τ that permitted a reasonably stable process when machining with copper electrodes was about 0,85 ($t_i = 300$ μ s, $t_o = 53$ μ s, $i_e = 40$ A). In this case, the

V_w was increased to 35,5 mm³/min and ϑ reduced to 2,4%, although the presence of a black film on the surface of both electrodes as well as a non-uniform tool electrode wear were observed. This effect was probably caused by insufficient time to expel the debris from the gap and consequently their over-concentration impelled the formation of arcing.

Figure 5b shows that for $i_e = 64$ A and 21 A, the V_w reached respectively 65,6 mm³/min and 16,6 mm³/min. The surface roughness of the parts did not change considerably because the discharge energy per pulse continued to be almost the same. However, using finishing machining settings where the magnitude of t_i is quite short, the best results were achieved with a duty factor τ of 0,5. For higher values of τ was observed the existence of arcing and in many situations a complete interruption of the process happened. For EDM with tungsten-copper electrodes using duty factors higher than 0,5 the process was quite unstable using both rough and finish parameters settings.

Test conditions:

roughing machining
workpiece: CuBe alloy tool-electrode: copper (+)
duty factor: variable $i_e : 40$ [A]

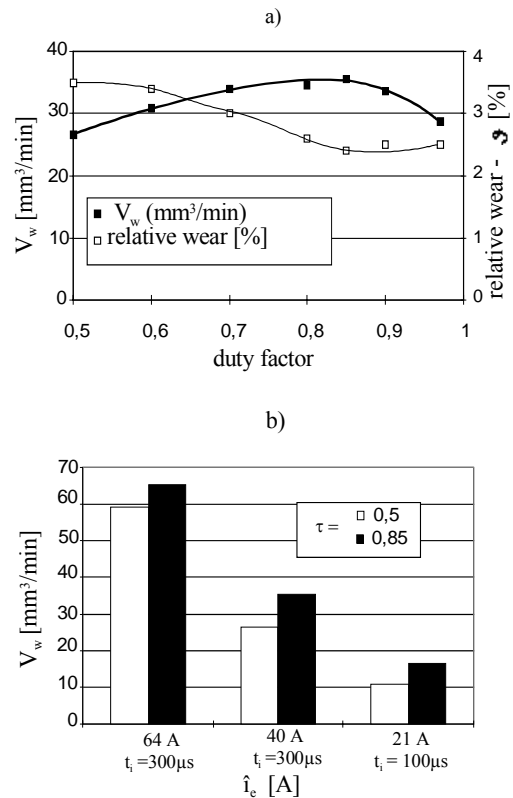


Figure 5. (a) Influence of duty factor τ , from 0,5 to 0,97, on the results of V_w and ϑ for copper electrode and $i_e = 40$ A (b) influence of $\tau = 0,5$ and $0,85$ on V_w for $i_e = 21, 40$ and 64 A at the optimum pulse duration t_i .

Barash (1965), Massarelli & Marchioni (1977), Jutzler (1982), Kruth et al. (1995) and König & Klocke (1997), among others research workers, have carried out studies to describe the structure and the mechanism of formation of the spark-affected surface layers produced on steels by electrical discharge machining. They present that when machining a workpiece with EDM a multilayered heat affected zone is created at the surface of workpiece. As an example, Fig. 6 from Amorim (2002) depicts the cross sectional view of an AISI P20 tool steel sample after EDM.

According to the cited researchers and VDI 3402 - Blatt 4 (2000) the heat affected zone created by EDM is constituted of an upper layer, known as either white layer or recast layer, followed by the phase transformation zone and the conversion zone.

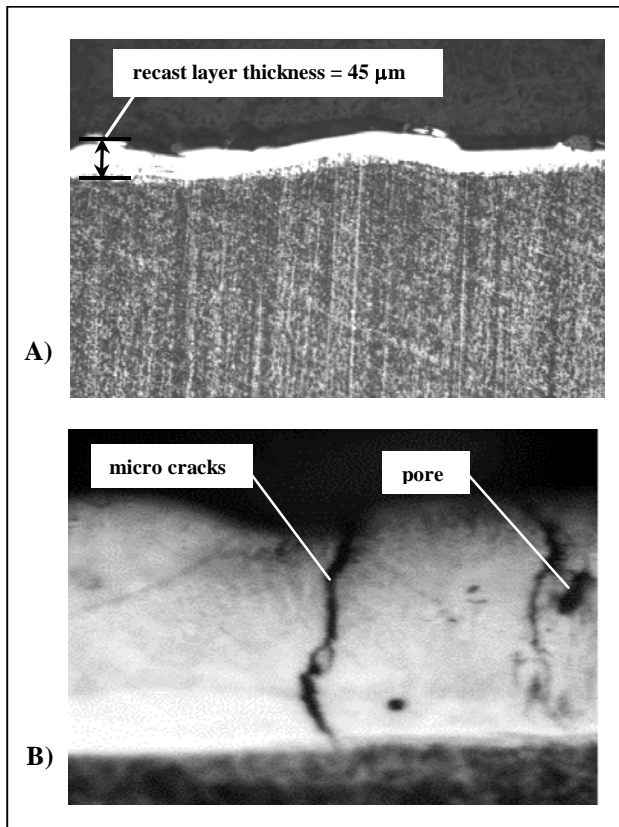


Figure 6. EDM sample of AISI P20 steel under $\hat{i}_e = 32$ A, $t_e = 400$ μs and $\tau = 0,8$. (A) Cross-sectional view showing the recast layer and (B) details of recast layer depicting micro-cracks and pores – magnified 50 times.

The recast layer is the outer region of the heat affected zone and consists of superimposed strata derived from melted and resolidified workpiece material. The structure of the recast layer that is formed on steels consists mainly of iron carbides in acicular or globular form, distributed within an austenite matrix, which are independent of the composition of the base material and of the type of the electrode, i.e., copper or graphite. The increase in carbon content in the recast layer is intrinsically related to the pyrolysis products that follows the cracking of the dielectric and is very confined to the melted and resolidified workpiece material forming the iron carbides. Due to the very high cooling gradient from the surface into the matrix material the iron carbides are normally oriented perpendicular to the surface. The high tensile surface stresses caused by the EDM phenomena also create pores and micro cracks perpendicular to the surface, as depicted in Fig. 6B. The micro cracks on steel workpieces are generally restricted to the recast layer.

Right below the recast layer comes the phase transformation zone, caused by heat of the EDM process, in which structural and chemical transformation occurred due to temperatures below the melting temperature of the material. The phase transformation zone usually consists of several layers, which are very difficult to be distinguished. In dependence of the material this zone may contain residual stresses, dislocations, slip lines, twin accommodations and also micro cracks. In case of steels the presence of a hardened layer

is normally noticed below the recast layer, which characterize the phase transformation zone.

Following the phase transformation zone is the conversion zone where changes in grain structure from the original structure is apparent. In steels the conversion zone is identified by a softened, annealed layer. Finally, appears the matrix material that has not undergone any thermal effect caused by the EDM process.

The optical microscope images depicted in Fig. 7 show the heat affected transverse layers of CuBe C17200 alloy under roughing and finishing machining. No micro cracks or pores are observed. It is clearly seen the existence of a recast layer on the surface of the workpiece, similar to the behavior of steel as shown in Fig. 6. This layer is caused by the material that was melted during the discharge and then when the discharge current breakdown occurred a part of the material has resolidified in the crater and surroundings and the rest was flushed away by the dielectric. Below the recast layer appears the matrix material, which seems not to be thermally affected.

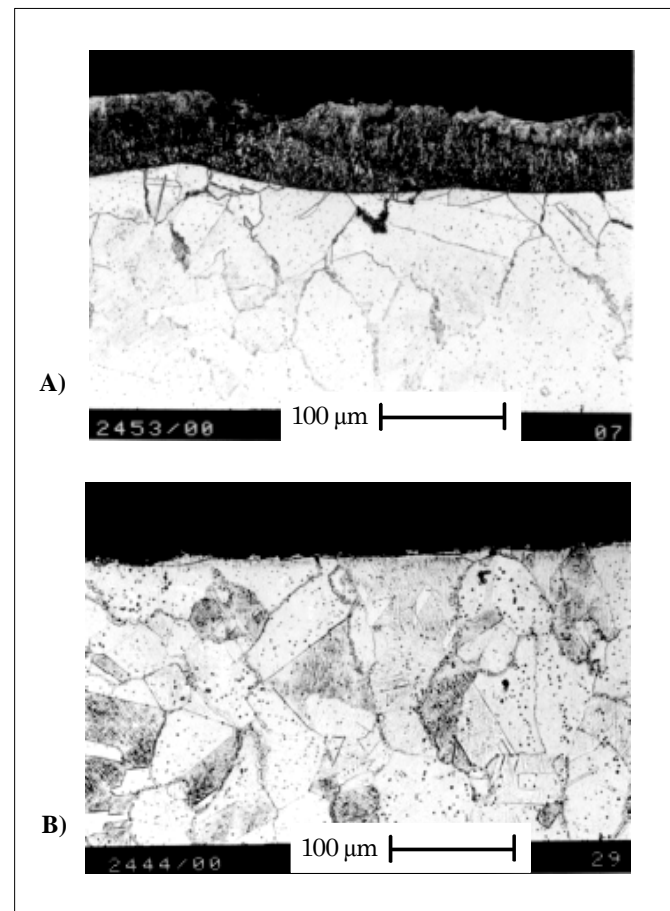


Figure 7. Transverse sections of CuBe samples after EDM. (A) rough machining under $\hat{i}_e = 64$ A, $t_e = 300$ μs, $\tau = 0,5$ depicting a 70 μm thickness dark recast layer and (B) finish machining under $\hat{i}_e = 4$ A, $t_e = 30$ μs, $\tau = 0,5$ depicting a very thin 5 μm thickness recast layer.

The depth of the recast layer was investigated by micro hardness measurements from 10 μm up to 220 μm below the surface for roughing regime and up to 60 μm for finishing regime, as presented in Tab 2. It was observed that the recast layer for finishing regime has a hardness of about 212 HV compared to approximately 489 HV encountered on the matrix material. For roughing regime the hardness measurements showed average values of 225 HV for the recast layer and 489 HV for the matrix material.

Table 2. Hardness measurement across transverse sections of CuBe alloy samples in rough and finish EDM.

Depth of Hardness Measurement [μm]	Hardness [HV]	
	Finishing	Roughing
10	212	205
15	476	216
20	487	236
30	486	228
60	495	241
110	-	398
130	-	435
150	-	459
220	-	489

From the analysis of microscope images in Fig. 7 along with its association with the values of Tab. 2, it is observed that the depth of the recast layer reaches about $70\ \mu\text{m}$ for roughing machining and for finishing machining the average depth is $5\ \mu\text{m}$, which is almost immeasurable in the micrographs due to the low discharge current applied in finishing regime. This fact emphasizes the expected relationship that increasing discharge current increases the depth of the recast layer, as also normally occurs in the case of steel workpiece samples.

Although a phase transformation zone and a conversion zone between the recast layer and the matrix material cannot be visually observed, their existences are evident by the gradual increasing in hardness through the depth of the transverse section, as shown in Tab.2. For finishing regimes is clearly seen from Tab.2 a high augment in hardness between 15 and $60\ \mu\text{m}$, which may be characterized as being the phase transformation zone followed by the conversion zone. The superior and inferior limits of that interval are therefore the probable boundaries of those to zones with the recast layer and matrix material. For roughing machining an expressive increase in hardness begins at about $110\ \mu\text{m}$ and reaches up to $220\ \mu\text{m}$, which is likely to be the phase transformation zone and the conversion zone. It can also be noted that higher is the discharge current more profound is the thermally affected zone.

According to Reed-Hill (1994) the high strength of CuBe alloys is to be obtained by age hardening or precipitation hardening of a beryllium-containing phase from a supersaturated solid solution of mostly pure copper. This precipitation occurs during the slow cooling of the alloy when the solubility of beryllium in copper decreases with decreasing temperature. Normally the precipitation or age hardening treatment takes about one hour or more at a temperature between 200 and $460\ ^\circ\text{C}$.

Basically, the phenomena of rapid resolidification of the material, that occurs after the electrical discharge is interrupted, may possibly explain the lower hardness of the recast layer in comparison with the hardness of matrix material after EDM. It means that there is not enough time to give rise to the beryllium-containing phases precipitation. As depicted by the SEM images in Fig. 8, the increase of surface roughness, which means that larger and deeper craters are produced on the surface of the part, is directly related to the increase in discharge current. The best results for the average roughness R_a of C17200 alloy, ranging from $1,0$ to $2,6\ \mu\text{m}$, are achieved for EDM under $i_c = 4, 8$ and $15\ \text{A}$ and $t_i = 30\ \mu\text{s}$, when the process was quite stable.

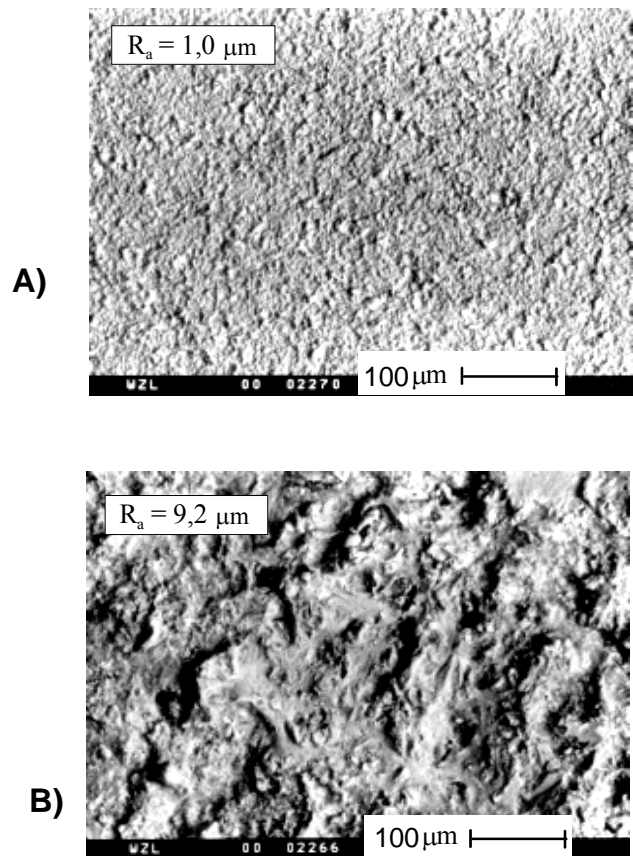


Figure 8. SEM images of the surface of CuBe samples depicting the increase of roughness with the elevation of discharge current i_c when (A) finish EDM at $i_c = 4\ \text{A}$, $t_i = 30\ \mu\text{s}$, $\tau = 0,5$ and (B) rough EDM under $i_c = 64\ \text{A}$, $t_i = 300\ \mu\text{s}$, $\tau = 0,5$.

As represented before in Fig.1, at the end of the pulse duration t_p , an interval time t_o is established in order to de-ionize the dielectric and flush away the material that has been melted during the time the plasma channel is sustained. As described by Dibitonto et al.(1989), during this period a violent collapse of the plasma channel and the vapor bubble occurs, subsequently causing the superheated molten liquid pool on the surface of both electrodes to be ejected into the liquid dielectric.

Lhiaubet & Meyer (1981) explain that the expelled material from the electrodes can be sorted in two basic categories. The first ones are solid spheroids resulted from the removal of liquid metal. The second category are hollow spheroids credited to be formed from the material expelled in a vapor phase, forming a bubble in the cool dielectric and because the rapid condensation takes the geometry of the bubble. The SEM micrograph in Fig. 9A shows the form of the debris particles resulted from the EDM of CuBe samples. It is observed that the majority of particles are spheroids of different sizes and some particles exhibit a wide variety of geometries and sizes. The phenomenon of coalescence of small droplets may in part explain the formation of the biggest spheroids as well as the random geometry debris particles.

The superimposed craters evidence the thermal nature of material removal process in EDM as shown in Fig. 9B.

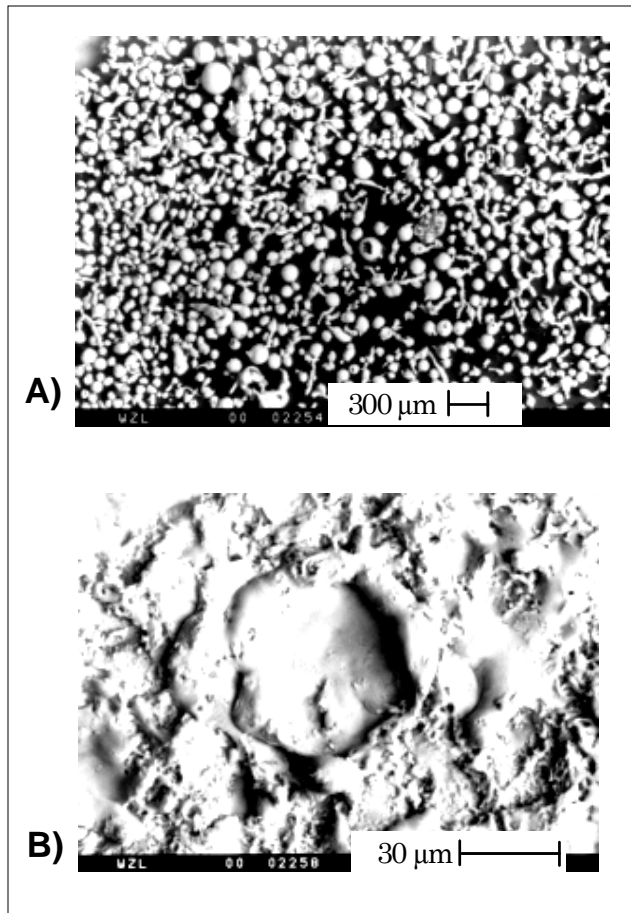


Figure 9. SEM images depicting (A) the form of debris particles of EDM and (B) the superimposed craters on the surface of a EDM CuBe sample.

Conclusions

From the experiments carried out in this study the following conclusions may be drawn:

a) The values of material removal rate V_w for CuBe C17200 alloy are lower than those normally found for EDM of steel workpieces. For instance, Amorim & Weingaertner (2003) report that when EDM AISI P20 steel samples, values of material removal rate V_w of approximately $90 \text{ mm}^3/\text{min}$ is usually reached for $t_c = 400 \text{ } \mu\text{s}$ and $\tau = 0,8$ using positive copper tool electrodes, which is much higher than the maximum V_w of about $65,6 \text{ mm}^3/\text{min}$ achieved for CuBe alloy under $i_c = 64 \text{ A}$, $t_i = 300 \text{ } \mu\text{s}$ and $\tau = 0,85$. The reason for such considerable difference is mainly related to the higher thermal conductivity of CuBe (105 W/mK) in comparison to AISI P20 steel (30 W/mK), which diminishes the material removal rate V_w .

b) The best results of V_w and surface texture for duty factor of 0,5 are obtained with tungsten-copper electrodes, no matter the machining condition.

c) The minimum surface roughness R_a of approximately $1,0 \text{ } \mu\text{m}$ was obtained for $i_c = 4 \text{ A}$, $t_i = 30 \text{ } \mu\text{s}$, $\tau = 0,5$

d) When EDM with tungsten-copper electrodes the increase of i_c promotes lower volumetric relative wear ϑ .

e) When EDM with copper electrodes the increase of i_c promotes higher level of ϑ .

f) The transverse section of EDM CuBe alloy samples consists of a recast layer followed by a phase transformation zone and a conversion zone, although these two last ones cannot be visually observed.

g) The depth of the recast layer, the phase transformation zone and the conversion zone increases with the raise of discharge current i_c and pulse duration t_i . The recast layer showed an average depth of $5 \text{ } \mu\text{m}$ for finish machining and $70 \text{ } \mu\text{m}$ for rough machining.

h) The presence of a phase transformation zone and a conversion zone, although they cannot be seen under optical microscope, is evidenced by the gradual increase in hardness through the transverse section of the samples.

i) No micro cracks or pores are observed across the recast layer and thorough the thermally influenced zones.

j) The surface roughness increases with both discharge current and pulse duration.

k) Hardness measurements showed that the recast layer is softer than the matrix material, presenting a hardness of 212 HV compared to 489 HV encountered on the matrix material.

References

- ACGIH, American Conference of Governmental Industrial Hygienists, 1995, "Industrial ventilation: a manual of recommended practice", 22nd edition, USA
- Amorim, F.L., 2002, "Technology for Die-Sinking EDM of AMP 8000 Aluminum Alloy and CuBe Copper-Based Alloy used as materials for Injection Molding Tools of Plastic Products" (in portuguese), doctoral thesis, Department of Mechanical Engineering, Federal University of Santa Catarina, Florianópolis, SC, Brasil.
- Amorim, F.L., Weingaertner, W.L. 2003 "Die-sinking EDM of AISI P20 tool steel under rough machining using copper electrodes" 2o. COBEF - Congresso Brasileiro de Engenharia de Fabricação, 18-21 Maio, Uberlândia, Brasil, CD-Rom, pp.1-5.
- Barash, M.M., 1965 "Effect of EDM on the surface properties of tool and die steels", Metal Engineering Quarterly, vol 5, No.4, pp.48-51.
- Crookall, J.R., Khor, b.C., 1974, "Electro-discharge surfaces", Proceedings of the Fifteenth International Machine Tool Design and Research Conference, September 18-20, England, Vol.1, pp. 373-384.
- Dibitonto, D.D., Eubank, P. T., Mukunk, R. P., Barrufet, M.A., 1989, "Theoretical models of the electrical discharge machining process I: a simple cathode erosion model", Journal of Applied Physics, Vol. 66, No. 9, pp. 4095-4103.
- Drozda, T.J. 1983, "Tool and manufacturing engineers handbook" SME, Dearbon, USA.
- Engellman, P., Deadey, B., 2000, "Maximizing performance using copper alloys", Modern Mold & Tooling, Vol. 2, No. 2, pp. 39-42.
- Guha, A., Smyers, S., Rajurkar, K. P., Garimella, P.S., Konda, R., 1995, Optimal parameters in electrical discharge machining of copper beryllium alloys, Proceedings of the International Symposium for Electromachining, Switzerland, vol. 1 pp. 217-224.
- Jutzler, W-I., 1982, "Funkenerosives senken - verfahrenseinflüsse auf die oberflächenbeschaffenheit und die festigkeit des werkstücks", doktoringenieurs dissertation, Fakultät für Maschinenwesen der Rheinisch-Westfälischen Technischen Hochschule Aachen, Deutschland.
- Klocke, F., 1998, "The process sequence in tool and diemaking", Proceedings of the International Symposium for Electromachining, May 11-13, Germany, Vol. 1, pp. 65-97.
- König, W., Klocke, F., 1997, "Fertigungsverfahren - 3: Abtragen und Generieren", Springer, Berlin.
- Kruth, J.-P., Stevens, L., Froyen, L., Lauwers, B., 1995 "Study of the white layer of a surface machined by die-sinking electro-discharge machining", Annals of CIRP, vol. 44, No. 1, pp.169-172
- Lhiaubet, C., Meyer, R. M., 1981 "Method of Indirect Determination of the Anodic and Cathodic Voltage Drops for Short High-Current Electric Discharges in a Dielectric Liquid" Journal of Applied Physics, Vol.52, No.6, pp. 3929-3934.
- Massarelli, L., Marchionni, M., 1977 "Morphology of spark-affected layers produced on pure iron and steels by electro-discharge machining", Metal Technology, vol.1, No.1, pp100-105.
- Reed-Hill, R.E., 1994 "Physical metallurgy Principles", 3rd. editions, PWS Publishing Company, USA.
- Stonehouse, A. J., 1986, Physics and chemistry of beryllium, J. Vac. Sci. Technol., vol. 4, n.3, pp. 1163-1170.
- Stevens, L. 1998, Improvement of surface quality in die-sinking EDM, doctoral thesis, Department of Mechanical Engineering, K.U. Leuven, Belgium.

Van Dijk, F., Crookal, J.R., Heuvelman, C. J., Snoyes, R. 1974, "Some Results of Physical Research in EDM", IV International Symposium for Electromachining, Vol.1, Bratislava, Poland, pp.68-85.

VDI - Verein Deutscher Ingenieure - 3402 - Blatt 4 -2000 "Anwendung der Funkenerosion" VEB, Verlag Technik, Berlin.

Zolotyck B. N.,1955 "Physikalische Grundlagen der Elektrofunktenerosion von Metallen", VEB, Verlag Technik, Berlin.